The effect of surface and hydrodynamic forces on the shape of a fluid drop approaching a solid surface

1996 J. Phys.: Condens. Matter 8 9483

(http://iopscience.iop.org/0953-8984/8/47/049)

J. Phys.: Condens. Matter **8** (1996) 9483–9490. Printed in the UK

The effect of surface and hydrodynamic forces on the shape of a fluid drop approaching a solid surface

R G Horn†, D J Bachmann, J N Connor and S J Miklavcic‡

Ian Wark Research Institute and School of Applied Physics, University of South Australia, The Levels, SA 5095, Australia

Received 5 July 1996, in final form 20 September 1996

Abstract. This paper describes an experiment designed to measure surface and hydrodynamic forces between a mercury drop and a flat mica surface immersed in an aqueous medium. An optical interference technique allows measurement of the shape of the mercury drop as well as its distance from the mica, for various conditions of applied potential, applied pressure, and solution conditions. This enables a detailed exploration of the surface forces, particularly double-layer forces, between mercury and mica. A theoretical analysis of drop shape under the influence of surface forces shows that deformation of the drop is a sensitive indicator of the forces, as well as being a very important factor in establishing the overall interaction between the solid and the fluid.

1. Introduction

The physical interactions of fluid drops with each other, with solid particles, or with solid surfaces, are very important in determining the behaviour of numerous systems such as emulsions, foams, and mineral flotation processes. While the surface forces acting between solids have been studied extensively in recent years and direct measurements have been made using surface force apparatus and atomic force microscope techniques, much less work has been done on interactions involving fluid interfaces. Clearly, the deformability of such interfaces will be an important factor in interactions involving fluid drops, whereas it is rarely an issue in colloidal interactions between solids. In addition, deformations caused by hydrodynamic pressure on a moving drop can be very significant, especially when the drop approaches another body.

In this paper we describe a combined theoretical and experimental approach to exploring how forces involving fluid drops are influenced by interfacial deformations. Initially our focus is on surface forces rather than hydrodynamic forces, and we consider the interaction between a non-aqueous fluid drop interacting with a flat solid surface, when both are immersed in an aqueous phase. A theoretical analysis presented in the next section illustrates some general features of interactions involving deformable drops. This is followed by a description of our experimental set-up, which allows measurements of forces, surface separations and drop deformations when a drop of mercury is brought close to a mica surface in water.

† To whom any correspondence should be addressed (e-mail: roger.horn@unisa.edu.au).
‡ Present address: Department of Physics and Measurement Technology, Linköping University, S-581-83 Linköping, Sweden.

0953-8984/96/479483+08$19.50

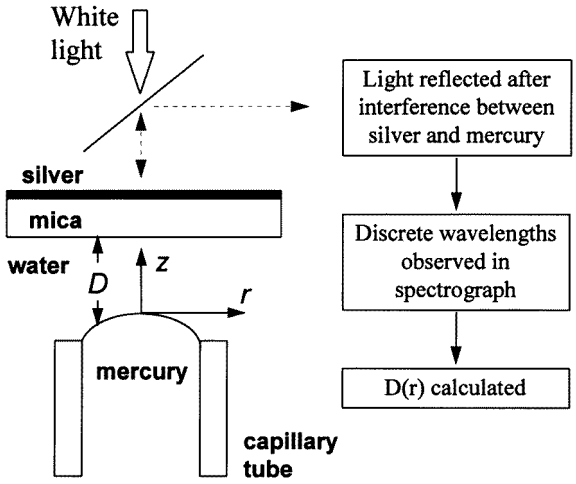

Figure 1. The experimental arrangement used to measure deformations in the shape of a mercury drop as it approaches a flat mica surface, when they are separated by an aqueous phase. Due to optical interference between the partially reflecting silver layer and the mercury, reflected light has (dark) fringes of equal chromatic order which are measured in an imaging spectrograph to yield $D(r)$.

2. Theoretical details

The shape of a fluid interface is established by the forces acting on it, which can include surface or interfacial tensions, gravitational forces and forces due to interaction with another object. Here we consider a protruding drop at the open end of a cylindrical capillary which is pointing vertically upwards. This configuration, shown in figure 1, corresponds to the experimental system to be described in the next section. Above the drop is a horizontal solid surface with which the drop may interact via surface forces, for example, electrical double-layer and van der Waals forces. The drop and the solid are immersed in a second fluid, which is less dense than the fluid in the drop.

From the Young–Laplace equation, the local curvature at any point on the drop's surface is determined by the pressure difference between the interior and the exterior of the drop. This can be expressed as [1, 2]

$$\gamma\left[\frac{z''(r)}{(1+z'(r)^2)^{3/2}}+\frac{z'(r)}{r(1+z'(r)^2)^{1/2}}\right]=\Delta\rho\, gz(r)+\Pi(r)-P_{app} \qquad (1)$$

where γ is the fluid–fluid interfacial tension, the two terms in the square brackets represent the principal curvatures orthogonal and parallel to the radial direction r, $\Delta\rho$ is the difference between the fluid densities, g is the gravitational acceleration, $\Pi(r)$ is the disjoining pressure, i.e., the pressure acting on the drop due to surface force interactions with the solid surface, and P_{app} is the pressure within the drop causing it to protrude from the capillary, measured immediately below the drop apex. The cylindrical polar coordinate system has its origin at the apex of the drop with the z-axis vertical and directed towards the solid surface, which lies in the plane $z = D_0$ (see figure 1).

In the absence of disjoining pressure, this is the equation describing the shape of a sessile drop. With disjoining pressure present due to a nearby solid surface, we invoke the Derjaguin approximation, and consider the disjoining pressure at the radial distance r to be

equal to that between flat plates at the separation $D(r)$,

$$\Pi(r) = \Pi(D(r)) = \Pi(D_0 - z(r)) \tag{2}$$

(since $z \leqslant 0$ for the convex sessile drop under consideration). For mercury interacting with a solid surface across an aqueous electrolyte solution, contributions to disjoining pressure will come from electrical double-layer forces and van der Waals forces. It is conceivable that there will be other forces present in this system, for example, solvation or hydrophobic forces, but for the present purposes of illustrating the general behaviour of the system, it is sufficient to consider a non-retarded van der Waals force and a simple form for double-layer pressure derived from the linear Poisson–Boltzmann equation [3] which, for surfaces having fixed potentials ψ_{01} and ψ_{02}, gives

$$\Pi(D) = \frac{\varepsilon\kappa^2}{2\sinh^2\kappa D}\left[2\psi_{01}\psi_{02}\cosh\kappa D - \psi_{01}^2 - \psi_{02}^2\right] - \frac{A}{6\pi D^3}. \tag{3}$$

In this equation ε is the dielectric permittivity of water, κ is the usual Debye parameter, and the last term is the van der Waals force, with A being the Hamaker function. A calculation using Lifshitz theory, with mercury represented [4] by a free-electron model having a plasma frequency of 1.66×10^{16} rad s^{-1}, gives $A = 4.0 \times 10^{-20}$ J at $D \to 0$.

Recently we have presented results from numerical solutions of equation (1) for symmetric [1] ($\psi_{01} = \psi_{02}$) and asymmetric [2] ($\psi_{01} \neq \psi_{02}$) double-layer interactions. Figure 2 shows some representative behaviour. In figure 2(a) the disjoining pressures are plotted for three combinations of surface potential: symmetric, asymmetric and antisymmetric. The deformation of the drop's surface under the influence of a disjoining pressure is illustrated in figure 2(b). At large separations (**A**) the drop is not greatly deformed by the disjoining pressure; at intermediate separations (**B**), where the disjoining pressure is repulsive, there is some flattening of the drop; and at small separations (**C**) where the surface force becomes attractive, the apex of the drop is drawn towards the solid and the drop shape becomes elongated.

From figure 2(b) it can be seen that profiles **B** and **C** cross each other: far from the apex, profile **C** lies between profiles **A** and **B**. It is illuminating to consider the separation between the solid and a remote part of the drop where its deformation due to disjoining pressure is negligible. In view of our experimental arrangement, a suitably remote part of the drop can be taken at the edge of the capillary, where the drop is pinned; the distance between the capillary and the solid is controlled experimentally. In figure 2(c) we plot the variation of the minimum separation as a function of the position of the 'grips' that hold the drop, i.e., the distance, D_c, between the solid and the end of the capillary, shifted by a constant z_c (the height of the drop in the absence of deformation due to disjoining pressure). In other words, the x-axis represents the position of the virtual apex of the undeformed drop, given by $D_u = D_c - z_c$. If the drop is flattened then we have $D_0 > D_u$, and if it is elongated then $D_0 < D_u$. It can be seen from figure 2(c) that when attractive surface forces are present at small separations (the dotted curve), there are two possible configurations D_0 for a given distance between the flat surface and the capillary. The lower value (such as profile **C**) is unstable, and the drop would be pulled into contact with the solid, flattening against it.

When the surface forces are repulsive and the pressure within the drop, P_{app}, does not exceed the maximum disjoining pressure, as indicated for the top curve in figure 2(a), the repulsive forces flatten the drop. It can be seen from equation (1) that when $\Pi(D_0) = P_{app}$, the curvature at the apex of the drop falls to zero. Pushing the drop towards the surface only increases the flattening and increases the total force acting between the drop and the solid, and the drop does not come closer to the solid than the separation D^*

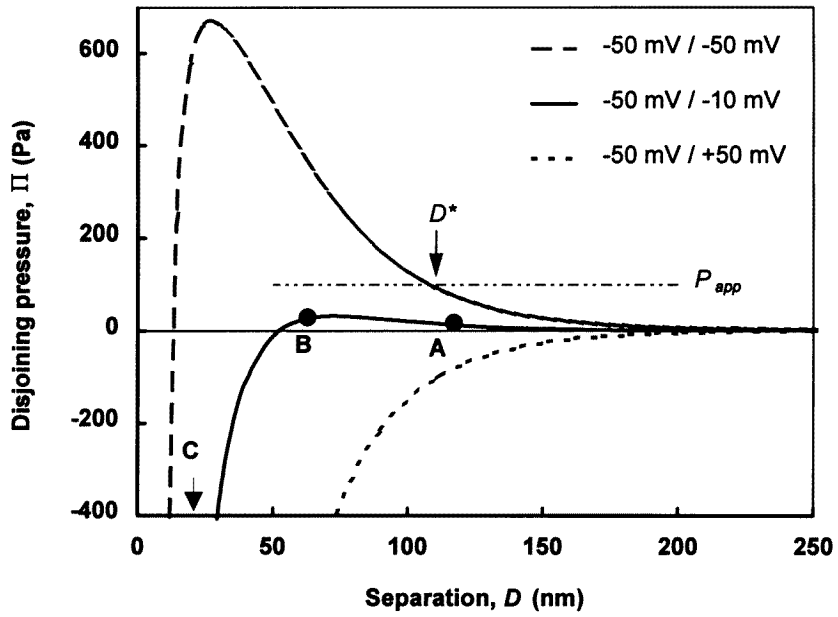

(a)

Figure 2. The effect of disjoining pressure (electrical double-layer and van der Waals forces) on the shape of the drop. (a) The disjoining pressure between flat surfaces computed from equation (3) for three different combinations of surface potential on the two surfaces: −50 mV/−50 mV (dashed line), −50 mV/−10 mV (full curve) and −50 mV/+50 mV (dotted curve), at a 1:1 electrolyte concentration of 1.0×10^{-4} mol l^{-1}. In the asymmetric case with two different potentials of the same sign, the pressure changes from repulsive at large separations to attractive at short separations, where there is charge reversal on the surface of lower potential [3]. A typical internal pressure in the drop, P_{app}, is indicated by the chain line. (b) Drop shapes computed from equation (1) for the case −50 mV/−10 mV with $P_{app} = 100$ Pa. Note that the vertical scale is much smaller than the horizontal scale, so the drop is much less curved than it appears in this figure. The drop flattens when the surface force at the apex is repulsive (profile **B**) and it is elongated when the force is attractive (profile **C**). (c) The variation of the minimum separation between the solid and the drop, D_0, compared to the distance D_u between the solid and the position of the virtual apex of the undeformed drop. When the disjoining pressure, e.g. at −50 mV/−50 mV, exceeds P_{app}, the drop flattens ($D_0 > D_u$) and the drop never gets closer to the solid than D^*, the separation at which $\Pi(D^*) = P_{app}$ (about 110 nm in this case). When P_{app} exceeds the maximum disjoining pressure, the D_0 versus D_u curve is re-entrant and the lower branch, where $dD_0/dD_u < 0$ (e.g. profile **C**), is unstable.

at which $\Pi(D^*) = P_{app}$. This result, discussed in detail in reference [1], clearly shows that deformation of a fluid drop has a dramatic effect on the total surface force acting on it. The significance of this effect for bubble–bubble interactions in water is examined in a forthcoming publication [5].

3. Experimental procedure

Our aim is to measure the deformation of a fluid drop under the influence of surface and hydrodynamic forces. Mercury is selected as the fluid, because (a) its reflectivity allows optical interferometry to be used to measure the shape and location of its surface; (b)

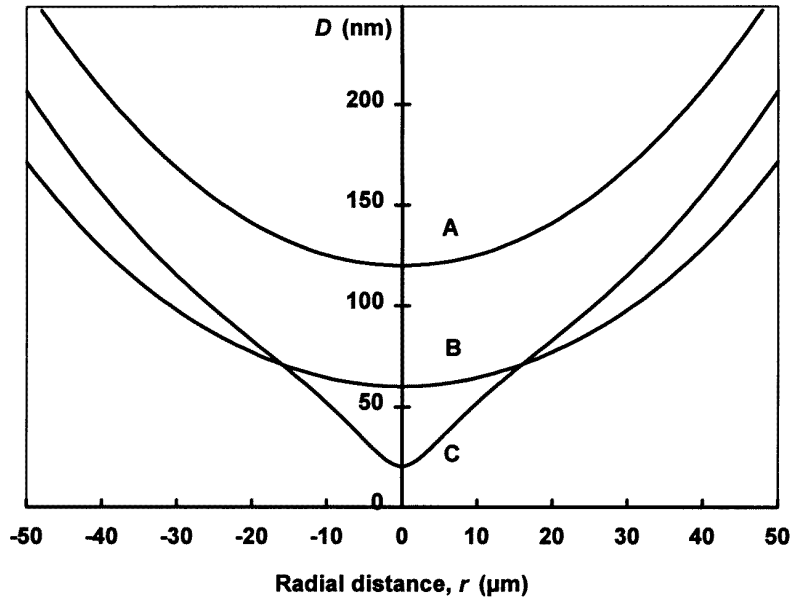

(b)

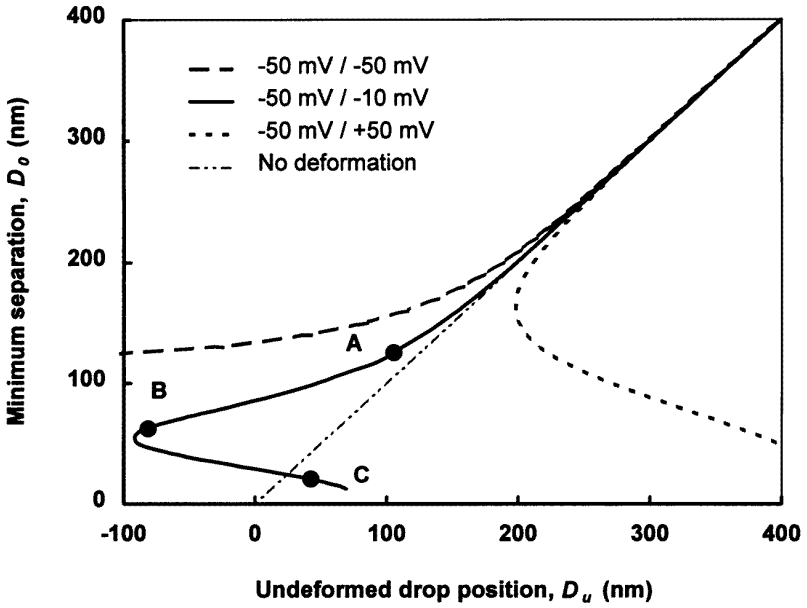

(c)

Figure 2. (Continued)

its conductivity allows control of its surface potential; and (c) a wealth of information is available on its surface charging behaviour in aqueous electrolyte solutions, from dropping mercury electrode (DME) experiments [6]. Mica is chosen as the solid because it has

a molecularly smooth surface, it can be prepared as very thin sheets of perfectly uniform thickness which are ideal for the optical interferometry method described below, and because its surface charging behaviour in aqueous solutions is known from numerous surface force apparatus studies [7].

As shown schematically in figure 1, mercury is introduced into a chamber filled with aqueous electrolyte, through a vertical capillary tube entering the bottom of the chamber. A small pressure ($\sim 10^2$ Pa) is applied so that the drop protrudes from the end of the capillary, while remaining pinned at the internal corner. The chamber and the capillary are both machined from Kel-F® (polychlorotrifluoroethylene), with the capillary having an internal radius of $\sim$1 mm. At the top of a chamber is a window, with a thin, horizontal sheet of mica glued to the lower surface. The window bearing the mica can be moved up and down with a two-stage differential-spring mechanism similar to that used in the SFA [8], allowing control of its position to better than 1 nm. The aqueous phase in the chamber is in contact with a reference electrode, with a second electrode contacting the mercury, so that the surface potential of the mercury may be varied. However, in the present series of experiments, no potentials were applied. Optical interference between a partially reflecting silver layer on the upper surface of the thin mica sheet and the surface of the mercury drop allows the mica–mercury distance and the shape of the mercury drop to be measured to high accuracy, employing fringes of equal chromatic order [8] observed in reflection.

Mercury is cleaned by washing in 10% nitric acid with agitation by bubbling oxygen, followed by rinsing with water from a Millipore MilliQ® system. The same water is used for experiments. The KCl is Analar grade from BDH. During experiments the surface of the drop is renewed immediately before each set of measurements by forcing more mercury through the capillary (with the mica moved far away) and spilling one or more drops to the bottom of the chamber.

4. Results and discussion

Some illustrative results obtained in water and in 1 mM KCl solution are shown in figure 3, in which data are plotted using the same axes as in figure 2(c), i.e. the minimum mica–mercury separation D_0 plotted as a function of the position D_u of the undeformed drop. These results were obtained by driving the mica slowly towards the fixed capillary at a constant speed, and subtracting the undeformed drop height from the capillary–mica distance to give D_u.

It can be seen that the two experimental curves qualitatively resemble the stable ($\mathrm{d}D_0/\mathrm{d}D_u > 0$) regions of two of the theoretical curves shown in figure 2(c). The curve measured in water corresponds to a purely attractive force (the dotted curve in figure 2(c)) with a measurable deformation of the drop detectable when $D_0 < 400$ nm. As D_0 decreases to below 200 nm the elongated drop configuration becomes unstable and the mercury is pulled abruptly into flat contact against the mica surface. In KCl there is some flattening of the drop ($D_0 > D_u$) between 400 and 100 nm, but below about 60 nm the drop is pulled into contact by an attractive force. This behaviour is like the solid curve in figure 2(c), corresponding to a repulsive force at long range becoming attractive at shorter range.

Since the range of the attractive force is significantly reduced when electrolyte is added to the water, the attraction can safely be ascribed to an electrical double-layer force. The repulsion observed in KCl is (most likely) not a surface force, but the effect of hydrodynamic pressure tending to flatten the drop. In water, the attractive force is of longer range, and it affects the drop shape at large D_0 where the hydrodynamic pressure (which is proportional to D^{-2}) is very small. However, when the double-layer attraction is screened by KCl, the hydrodynamic pressure is significant at separations up to 400 nm, and it flattens the drop

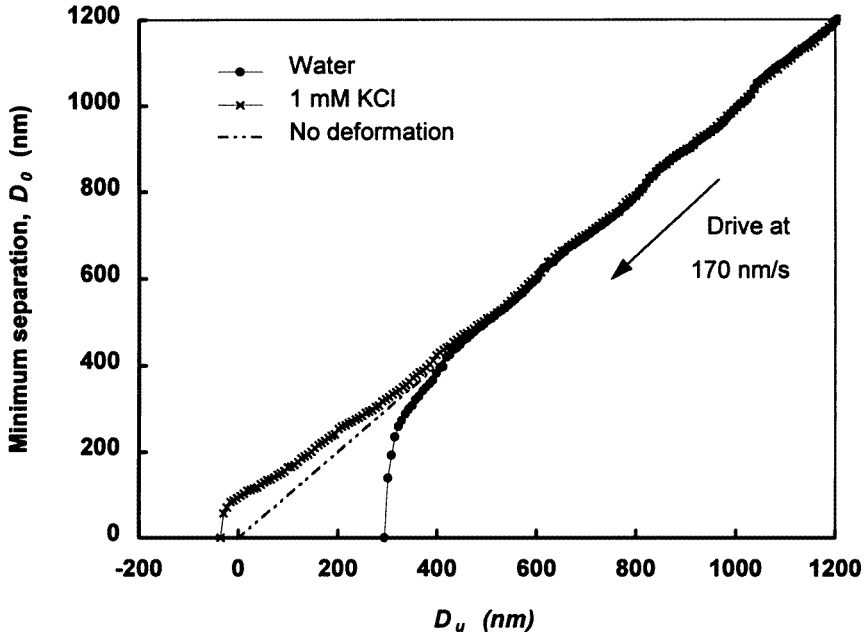

Figure 3. The minimum mercury–mica separation D_0 plotted as a function of the undeformed position D_u measured in water and in 1 mM KCl solution, with no potential applied to the mercury. These measurements were obtained by driving the mica surface towards the fixed capillary at a constant speed of 170 nm s^{-1}. In water, the deformation (elongation, $D_0 < D_u$) and the abrupt collapse to the mercury–mica contact ($D_0 = 0$) indicates an attraction between the mercury and mica; the electrolyte dependence suggests this is a double-layer force. In KCl there is some flattening ($D_0 > D_u$) due to hydrodynamic forces before the attractive force pulls the drop into contact with the solid.

before the attractive force becomes dominant at $D_0 < 100$ nm.

Our theoretical analysis of drop deformation under the influence of surface forces shows that measurable deformations occur with quite weak and long-range forces. The decay length $1/\kappa$ for the forces shown in figure 2(a) is 30 nm; figure 2(c) shows that the deformation is significant at distances many times larger than this, even for weak forces such as in the -50 mV/-10 mV case. The sensitivity of the drop shape to surface forces is confirmed by our experiments, where deformation is clearly evident at 400 nm in water. In effect, the drop itself is acting as a weak (and not necessarily linear) spring whose deformation serves to detect the force. Theoretical calculations as described in section 2 indicate that for small deformations the effective 'spring constant' is comparable to the mercury–water interfacial tension (0.43 N m^{-1}). The experimental results have the same qualitative form as the theoretical curves, but a detailed analysis is made difficult by the presence of a hydrodynamic pressure when the drop is moving towards the solid. This pressure is itself a very important factor affecting the approach of a fluid drop to a solid surface, and our future experiments will endeavour to separate the disjoining pressure from hydrodynamic pressure (by varying the applied potential and the speed of approach), in the hope of measuring both.

The observation of an attractive double-layer force, without any repulsion to prevent the mercury from coming into contact with mica, is in contrast to the results of Gupta and Sharma [9], who measured repulsive disjoining pressures between mercury and a

silica surface across salt solutions, by applying an appropriate potential to the mercury to give a repulsive double-layer force. Those authors also report a repulsive hydration force between mercury and silica, whereas no such force is observed here. A short-range hydration repulsion is generally observed between two silica surfaces interacting in aqueous solutions at all electrolyte concentrations [10], whereas a comparable force is only observed between mica surfaces at electrolyte concentrations higher than those employed in the present experiments.

In summary, we have presented a description of an experiment designed to measure surface and hydrodynamic forces between a mercury drop and a flat solid surface. Initial results show that weak, long-range forces can be detected with this technique. Theoretical analysis of the interplay between surface forces and deformation of the fluid drop shows a rich variety of behaviour [2] and indicates that deformation is a very important consideration. This may have far-reaching implications for the proper consideration of colloidal interactions between fluid drops.

Acknowledgment

We are grateful to the Australian Research Council for financial support of this work.

References

[1] Miklavcic S J, Horn R G and Bachmann D J 1995 *J. Phys. Chem.* **99** 16 357
[2] Bachmann D J and Miklavcic S J 1996 *Langmuir* **12** 4197
[3] Hunter R J 1987 *Foundations of Colloid Science* vol 1 (Oxford: Clarendon) ch 7
[4] See, for example, chapter 4 of reference [3].
[5] Miklavcic S J 1996 *Phys. Rev.* E at press
[6] See, for example,
Mohilner D M and Kakiuchi T 1981 *J. Electrochem. Soc.* **128** 350
or chapter 6 of reference [3].
[7] Pashley R M 1981 *J. Colloid Interface Sci.* **83** 531
[8] Israelachvili J N and Adams G E 1978 *J. Chem Soc. Faraday Trans.* I **74** 975
[9] Gupta A and Sharma M M 1992 *J. Colloid Interface Sci.* **149** 392, 407
[10] Horn R G, Smith D T and Haller W 1989 *Chem. Phys. Lett.* **162** 404